Physica B: Physics of Condensed Matter 530 (2018) 290–294

Contents lists available at ScienceDirect

Physica B: Physics of Condensed Matter

journal homepage: www.elsevier.com/locate/physb

Composition dependent cation distribution in $Zn_xGa_2O_{3+x}$ nanocrystals

Nannan Li, Pengfei Zhu, Xiulan Duan *

State Key Laboratory of Crystal Materials, Institute of Crystal Materials, Shandong University, Jinan 250100, PR China

ARTICLE INFO

Keywords:
A. Nanostructures
B. Luminescence
B. Microstructure
C. Photoelectron spectroscopy
C. Transmission electron microscopy (TEM)

ABSTRACT

$Zn_xGa_2O_{3+x}$ ($0.8 \leq x \leq 1.1$) nanocrystals with the size of 15–30 nm were prepared by the sol-gel method. The effect of composition (Zn/Ga ratio) on the distribution of Zn^{2+} and Ga^{3+} ions was studied using X-ray photoelectron spectroscopy (XPS). Both of these cations occupied tetrahedral sites as well as octahedral sites of spinel structure in the studied samples. Octahedral Ga^{3+} ions are dominant and the as-synthesized samples are partially inverse spinel-structure. The fraction of tetrahedral Ga^{3+} ions was calculated to be 0.07–0.16, and increased with Zn/Ga ratio increasing. The inverse parameter (two times the fraction of Ga^{3+} in the tetrahedral sites) increases from 0.14 to 0.32 when x value increases from 0.8 to 1.1. The EPR and emission spectra indicated that oxygen vacancies formed in the nanocrystals. The emission intensity of the peak due to oxygen vacancies decreased with increasing Zn/Ga ratio, indicating the decreasing of the concentration of oxygen vacancy.

1. Introduction

$ZnGa_2O_4$ is a kind of oxide phosphors and has better chemical and thermal stability under high electric field and high vacuum conditions compared to the sulfide phosphors [1–3]. $ZnGa_2O_4$ phosphor has attracted much attention because of its excellent luminescent properties and wide applications in vacuum fluorescent display (VFDs), field emission display (FEDs) and electroluminescent devices (ELDs) [4–7]. With the bandgap energy of 4.4–5.0 eV, $ZnGa_2O_4$ can exhibit ultraviolet and blue emission due to the transition via a self-activation center of Ga—O groups under the excitation of ultraviolet or low voltage electrons [8,9]. Furthermore, $ZnGa_2O_4$ shows various emission colors from green to red when doped with transitional metal or rare earth ions [10–13].

$ZnGa_2O_4$ belongs to mixed spinel structure, in which the oxygen ions arrange in close packed cubic structure forming tetrahedral and octahedral vacancies, Zn^{2+} and Ga^{3+} cations occupy one-half the octahedral sites and one-eighth of the tetrahedral sites. The distribution of Zn^{2+} and Ga^{3+} cations in the tetrahedral and octahedral sites of spinel structure is influenced by many factors, such as preparation method, temperature, composition of materials [14,15]. The cation distribution can be characterized by the inversion parameter y, which is defined as 2 times the fraction of Ga^{3+} ions in the tetrahedral sites (or the fraction of Zn^{2+} ions in the octahedral sites) [16]. The change of cation distribution in structure of spinel will have great effect on the optical properties of materials.

$ZnGa_2O_4$ was usually synthesized through solid-state reaction at high temperature [17,18]. In the present work, we prepared $Zn_xGa_2O_{3+x}$ nanocrystals with different composition by sol-gel method. X-ray photoelectron spectroscopy was used to study the distribution of Zn^{2+} and Ga^{3+} cations in the tetrahedral and octahedral sites and its influence by Zn/Ga ratio. The effect of Zn/Ga ratio on the emission properties was also studied.

2. Experimental

2.1. Preparation

The $Zn_xGa_2O_{3+x}$ ($x = 0.8$–1.1) nanocrystals were prepared by sol-gel method. Different amount of $Zn(OAc)_2.2H_2O$ and $Ga(NO_3)_3.\ xH_2O$ ($x = 5.75$) were firstly dissolved in deionized water. Citric acid was then added into the above solution as a chelating agent. The final solution was stirred for 1 h using a magnetic stirrer and then heated until highly viscous gels were formed. The gels were dried in an oven at 150 °C for 8 h followed by calcination at 600 °C for 2 h. Finally the $Zn_xGa_2O_{3+x}$ nanocrystals were obtained.

2.2. Characterization

Powder X-ray diffraction (XRD) patterns were carried out on a Rigaku D/Max-rA diffractometer using a Cu Kα radiation ($\lambda = 0.15418$ nm) and a graphite monochromator. Transmission electron micrographs (TEM) were recorded with a JEM-2100 microscope. X-ray photoelectron spectra (XPS) were measured using a Thermofisher ESCALAB 250 spectrometer

---

* Corresponding author.
E-mail address: xlduan@sdu.edu.cn (X. Duan).

https://doi.org/10.1016/j.physb.2017.11.047
Received 23 October 2017; Received in revised form 16 November 2017; Accepted 16 November 2017

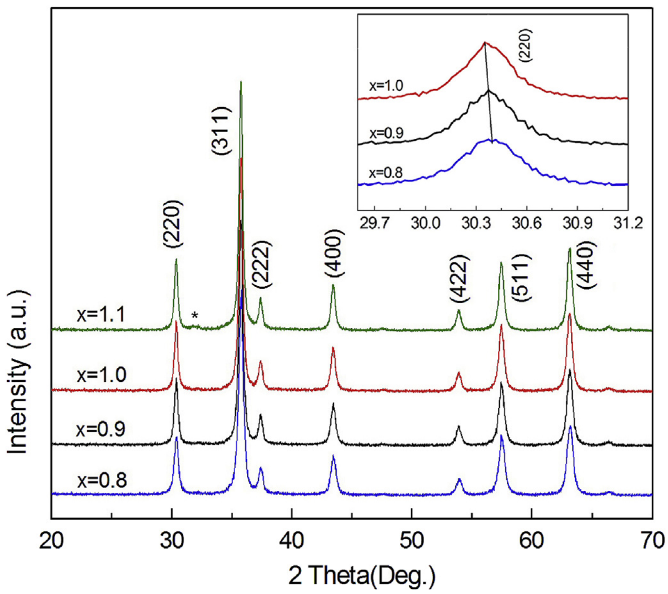

Fig. 1. XRD patterns of $Zn_xGa_2O_{3+x}$ nanocrystals annealed at 600 °C.

with monochromatized Al Kα radiation under ultrahigh vacuum (<10-7 Pa). The binding energies were calibrated using C1s peak (284.6 eV) as a reference. All the peaks were deconvoluted after background subtraction using a mixed Gaussian–Lorentzian function. Electron paramagnetic resonance spectrum (EPR) was detected on an ER200-D-SRC paramagnetic resonance spectrometer. Photoluminescence spectra were recorded using a FLS900 fluorescence spectrophotometer.

3. Results and discussion

3.1. Synthesis and morphology of $Zn_xGa_2O_{3+x}$ nanocrystals

The XRD patterns of $Zn_xGa_2O_{3+x}$ ($x = 0.8$–1.1) nanocrystals annealed at 600 °C were shown in Fig. 1. The peaks indexed as (220), (311), (222), (400), (422), (511) and (440) crystal planes in the XRD patterns were consistent with those of cubic $ZnGa_2O_4$ spinel (JCPDS No. 38–1240). ZnO impurity phase (marked as "*") appeared when the zinc precursor was superfluous. However, Ga_2O_3 phase was not detected when $0.8 \leq x \leq 1.0$. Moreover, the diffraction peaks of samples slightly shifted toward the lower diffraction angle with the increase of Zn content when $x \leq 1.0$. These results indicated that excess Ga_2O_3 dissolved into $ZnGa_2O_4$ phase to form solid solution. Therefore, the obtained samples were not the simple mixture of Ga_2O_3 and $ZnGa_2O_4$ but the homogenous $Zn_xGa_2O_{3+x}$ solid solution nanocrystals. The intensity of the diffraction peaks slightly increased with x value, indicating that zinc content increasing helped improve the crystallinity of $Zn_xGa_2O_{3+x}$.

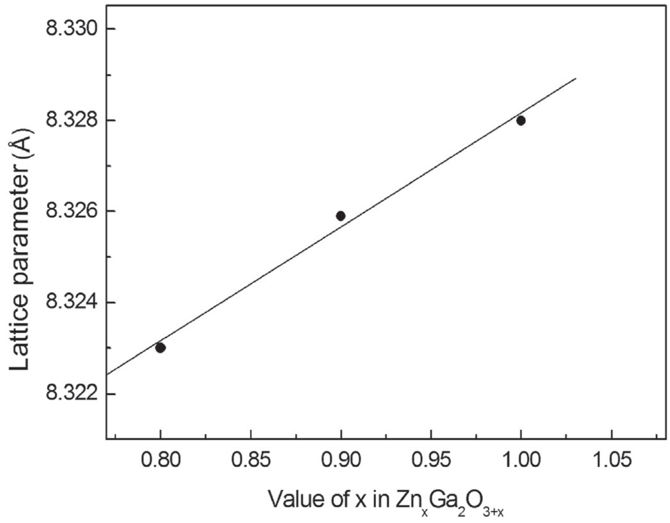

Fig. 2. Lattice parameter of $Zn_xGa_2O_{3+x}$ nanocrystals as a function of the Zn concentration.

The lattice parameter of the samples was calculated according to the XRD data and the parameter-composition relation is displayed in Fig. 2. It indicated the lattice parameter increased linearly with the increase of zinc content when Zn/Ga ratio is no more than 1.0. This trend is consistent with Vegard's law, which also confirms the formation of solid solution.

The TEM images of $Zn_xGa_2O_{3+x}$ nanocrystals are displayed in Fig. 3. All the samples were irregular spherical shape and the particles seriously agglomerated. The size of the particles was about 15–30 nm and increased with the increase of zinc content. The radius of Zn^{2+} (74 p.m.) is larger than that of Ga^{3+} (62 p.m.). The lattice parameter of $Zn_xGa_2O_{3+x}$ nanocrystals will increase with increasing Zn^{2+} content, which may result in the increasing particle size.

3.2. XPS studies

To study the influence of Zn/Ga ratio on the cation local environments in $Zn_xGa_2O_{3+x}$ nanocrystals, the XPS core level spectra of Ga $2p_{3/2}$ and Zn $2p_{3/2}$ were collected and shown in Fig. 4. It can be seen from Fig. 4a that all the Ga $2p_{3/2}$ spectra are relatively broad and asymmetric, and can be deconvoluted into two peaks through Gaussian-Lorentzian curve fitting, indicating that Ga^{3+} ions occupy two different coordination sites in $Zn_xGa_2O_{3+x}$. The peaks located at higher binding energy (~1118.3 eV) can be attributed to the Ga^{3+} ions at the octahedral sites and the weak peak at ~1116.6 eV can be due to tetrahedral Ga^{3+} ions [19,20]. Octahedral Ga^{3+} ions are dominant in all the studied samples, so we think that the as-synthesized samples are partially inverse spinel-structure.

Based on the element sensitivity factor method, the relative content of two elements can be calculated according to the following formula:

$$\frac{n_1}{n_2} = \frac{I_1}{I_2} \cdot \frac{S_2}{S_1} \tag{1}$$

where n_i, I_i and S_i are the concentration of atoms of element i, the XPS peak areas after background correction, and the empirically derived atomic sensitivity factors for an energy analyzer whose transmission function varies with the inverse of the electron kinetic energy, respectively [21–24]. For the same element located at two different environments, the parameter S_i keeps unchanged, and the above formula can be simplified as:

$$\frac{n_1}{n_2} = \frac{I_1}{I_2} \tag{2}$$

Therefore, the fraction of Ga^{3+} ions in these two sites can be estimated according to their concentration ratio of Ga_{tetra}/Ga_{octa}, which was calculated using Formula (2). The detailed data are shown in Table 1. It indicates that the fraction of tetrahedral Ga^{3+} ions is 0.07 when $x = 0.8$ and increases to 0.16 when $x = 1.1$. The inverse parameter (two times the fraction of Ga^{3+} in the tetrahedral sites) increases from 0.14 to 0.32 when x value increases from 0.8 to 1.1 (see Table 1).

The Zn $2p_{3/2}$ spectra (shown in Fig. 4b) are also asymmetric and can be deconvoluted into three peaks. The peak located at ~1023 eV can be assigned to octahedral Zn^{2+} ions and the peak at ~1022 eV is corresponding to tetrahedral Zn^{2+} ions. The third peak at about 1020 eV may be due to an impurity [25,26]. The fraction of octahedral Zn^{2+} ions also increases with zinc content increasing (Table 2).